Physica B 486 (2016) 60–63

Contents lists available at ScienceDirect

Physica B

journal homepage: www.elsevier.com/locate/physb

Period-doubling bifurcation cascade observed in a ferromagnetic nanoparticle under the action of a spin-polarized current

Paul P. Horley [a,*], Mykola Ya. Kushnir [b], Mishel Morales-Meza [a], Alexander Sukhov [c], Volodymyr Rusyn [b]

[a] Centro de Investigación en Materiales Avanzados, S.C. (CIMAV), Chihuahua/Monterrey, 120 Avenida Miguel de Cervantes, 31109 Chihuahua, Mexico
[b] Yuri Fedkovych Chernivtsi National University, 2 Kotsyubynsky str., 58012 Chernivtsi, Ukraine
[c] Institut für Physik, Martin-Luther Universität Halle-Wittenberg, 06120 Halle (Saale), Germany

ARTICLE INFO

Article history:
Received 20 May 2015
Received in revised form
11 November 2015
Accepted 5 December 2015
Available online 9 December 2015

Keywords:
Magnetization dynamics
Hysteresis
Bifurcation
Self-organization

ABSTRACT

We report on complex magnetization dynamics in a forced spin valve oscillator subjected to a varying magnetic field and a constant spin-polarized current. The transition from periodic to chaotic magnetic motion was illustrated with bifurcation diagrams and Hausdorff dimension – the methods developed for dissipative self-organizing systems. It was shown that bifurcation cascades can be obtained either by tuning the injected spin-polarized current or by changing the magnitude of applied magnetic field. The order–chaos transition in magnetization dynamics can be also directly observed from the hysteresis curves. The resulting complex oscillations are useful for development of spin-valve devices operating in harmonic and chaotic modes.

1. Introduction

Nano-scale magnetics attracted a considerable scientific attention, largely fueled by the discovery of the giant magnetoresistance [1,2] that was instrumental for significant increase of information storage density [3,4]. The elementary spintronic device, a spin valve, features high sensitivity to magnetic fields and short response time, which makes it promising for fast non-contact magnetic sensor applications [5]. The injection of spin-polarized current generates a spin torque [6] that produces a complex magnetization precession [7–10]. The careful tailoring of external influence in a form of pulsed fields and currents leads to a rich variety of dynamic states displayed by a spin valve, including ultrafast reversal under pulsed magnetic field [11,12], steady magnetization precession and canted states [13], as well as complex magnetization dynamics triggered with pulsing currents [14]. The increase of device operation temperature [15] leads to stochastic oscillations and chaotic states, which can be useful for generation of true random numbers [16]. To increase power output of a spintronic device, several nano-magnets can be synchronized, leading to a variety of coupling effects [8,17]. It was shown that the methodology developed for characterization of self-organizing dissipative systems [18] can be successfully applied for study of complex dynamic modes appearing in nano-magnetic systems [19–21]. The accounting for such non-linear magnetic behavior is important, as it may lead to spin wave instabilities [22], chaotic vortex core reversal [23] and related phenomena.

In this paper, we report on cascades of period-doubling bifurcations occurring in a macrospin model describing magnetization dynamics of a free layer in Co/Cu/Co spin-valve [7], subjected to simultaneous action of a constant spin-polarized current and periodic external magnetic field. We use bifurcation diagrams and Hausdorff dimension as main tools to visualize the different magnetic oscillation modes. We also show that period doubling bifurcations are clearly detectable directly from the hysteresis curves, which opens new perspectives for experimental observation of order–chaos transition in spintronic devices.

2. Theoretical model

To study magnetization dynamics in relatively large particles, it is imperative to use micromagnetic simulations [24,25], dividing the object into small domains that interact with each other. However, dynamics of a thin free magnetic layer can be described reasonably well in the framework of macrospin approximation [9,26], when uniform magnetization rotation predominates in the system [27]. The calculations made with macrospin model reveal magnetization precession modes with the frequency distribution closely related to the experimental data [7]. Moreover, the

* Corresponding author.
E-mail address: paul.horley@cimav.edu.mx (P.P. Horley).

http://dx.doi.org/10.1016/j.physb.2015.12.010
0921-4526/

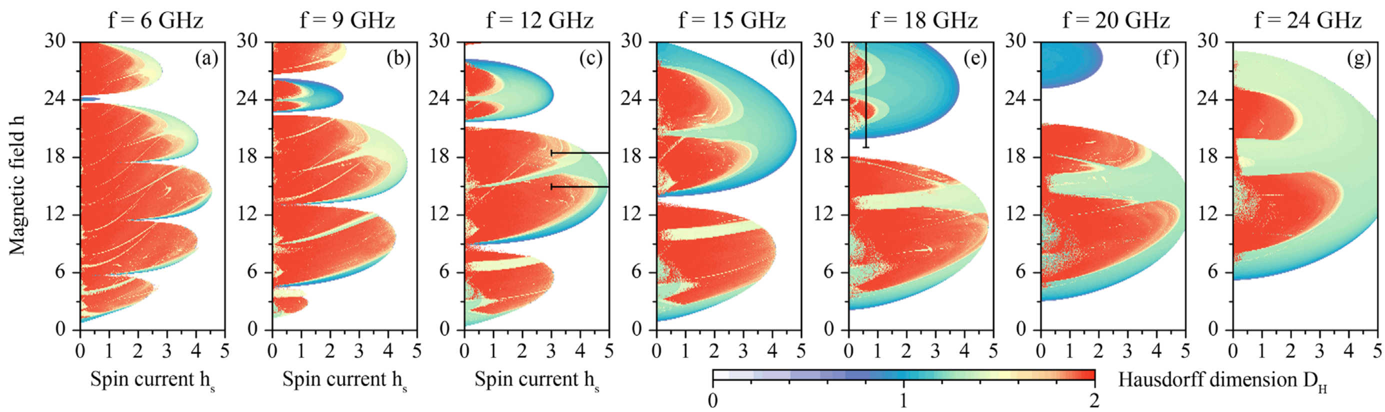

Fig. 1. "Synchronization islands" revealed with Hausdorff dimension D_H for magnetic field frequencies varying from 6 GHz (panel (a)) to 24 GHz (panel (g)). Panel (f) was calculated for 20 GHz to illustrate an island located at $h>24$, which is no longer observable at f=21 GHz. The dark bars in panels (c) and (e) correspond to parameter ranges used for the bifurcation diagrams shown in Figs. 2–4.

coherent magnetic rotation provides higher coercivity values in comparison with curling and multi-domain states [28]. Therefore, macrospin approximation became the main model considered for the spin-torque oscillators [29,30]. The magnetization dynamics in this case obeys the Landau–Lifshitz–Gilbert equation [31,32]:

$$\frac{d\vec{M}}{dt} = -\gamma\mu_0(\vec{M}\times\vec{H}) + \frac{\alpha(\xi)}{M_S}\left(\vec{M}\times\frac{d\vec{M}}{dt}\right) + \frac{\gamma}{M_S}[\vec{M}\times(\vec{M}\times\vec{J})]. \quad (1)$$

Here, γ is the gyromagnetic ratio, μ_0 is the vacuum permeability, M_S is the saturation magnetization and $\alpha(\xi)$ is the viscous damping coefficient [32]. The last term in Eq. (1) corresponds to the adiabatic spin torque proposed by Slonczewski [6] and Berger [33], caused by the injected spin-polarized current and counteracting magnetization precession damping. The non-adiabatic [34] field-like torque $\frac{\gamma\beta_S}{M_S}(\vec{M}\times\vec{J})$ was not considered in this study because of its smallness in the model spin valve system due to vanishing transverse magnetic coherence length [35,36]. As Eq. (1) unconditionally preserves the longitude of magnetization vector, it is useful to rewrite it in dimensionless variables for spherical coordinate system defined by the angles θ and φ [37]:

$$\frac{d\theta}{d\tau} = -\sin\theta(\alpha(\xi)A - B), \quad \frac{d\varphi}{d\tau} = \alpha(\xi)B + A \quad (2)$$

where

$$A = Z(\varphi)\cos(\theta) + h, \quad B = \tfrac{1}{2}h_p\sin 2\varphi + h_s$$
$$Z(\varphi) = (1 + h_p\cos^2\varphi), \quad \tau = t\gamma H_k/(1+\alpha(\xi)^2). \quad (3)$$

The reduced variables include: the time coefficient $\tau = t/[(1+\alpha(\xi)^2)/(\gamma\mu_0 H_k)]$, the anisotropy coefficient $h_p = K_p/K$ (with easy axis and easy plane anisotropy constants K and K_p, respectively), as well as dimensionless spin-current torque $h_s = (\hbar\eta J)/(4eVK)$ defined with spin-polarization degree η and the volume of ferromagnetic body V. The applied field was normalized over the uniaxial anisotropy $H_k = 2K/M_S$. We used material parameters for cobalt [28], with $K_p = 10$ kOe and $H_k = 500$ Oe [7]. To replicate the experimental setup, the free layer of a spin valve was considered to be a thin elliptic cylinder $130\times 70\ \mathrm{nm}^2$ in cross-section and 3 nm thick [7]. To improve model accuracy, we used the enhanced angle-depending formula for the damping coefficient $\alpha = \alpha_0(1 + q_1\xi + q_2\xi^2 + \cdots)$ as proposed by Tiberkevich and Slavin [38]. The parameter ξ depends on orientation of magnetic vector as

$$\xi = \frac{\alpha_0^2(1+\alpha_0^2)}{\gamma^2 H_k^2 M_S^2}\left(\frac{d\vec{M}}{dt}\right)^2 = \alpha_0^2(A^2+B^2)\sin^2\theta. \quad (4)$$

The equilibrium value for Gilbert damping coefficient was $\alpha_0 = 0.014$; the coefficients $q_{1,2}$ for Taylor series expansion were considered equal to 0.5.

3. Results and discussion

Eqs. (2) and (3) were solved with Runge–Kutta method of the fourth order [39] with integration step of 1 ps. The reduced magnetization $\vec{m} = \vec{M}/M_S$ was reconstructed from $\theta(\tau)$, $\varphi(\tau)$ as

$$m_x = \sin\theta\cos\varphi, \quad m_y = \sin\theta\sin\varphi, \quad m_z = \cos\theta. \quad (5)$$

To trigger complex magnetization precession modes, we used harmonic magnetic field $h = h_0\cos(2\pi f t)$ varying with a frequency f. Due to the complex nature of torque produced by h and h_s, both applied along z-axis, it was found that magnetization component m_z featured smaller amplitude in comparison with components m_x and m_y that are perpendicular to the direction of the field. Due to this, we chose m_x component for plotting the hysteresis curves.

To define parameter regions where magnetization precession takes place, we calculated Hausdorff dimension [18]

$$D_H = \lim_{\varepsilon\to 0}\frac{\log N}{\log\varepsilon^{-1}}, \quad (6)$$

where N is the number of cubes with the side ε required to cover the entire phase trajectory. As LLG equation describes magnetization dynamics restricted to a sphere, the possible values of D_H vary between the unity (steady precession) to two (chaotic oscillations covering the entire surface of the sphere). When the combination of control parameters fails to excite precession, the Hausdorff dimension tends to zero. Plotting the values of D_H as a function of h and h_s for a given field frequency f, one can clearly distinguish parameter regions corresponding to established magnetization precession from the parameter combinations for which the system converges to a fixed stationary state (Fig. 1). We will use the term "synchronization islands" to designate the areas in parameter space for which magnetization precession is achieved. The ranges of field frequency was chosen to include the characteristic frequency of the system $f_0 = (\gamma\mu_0 H_k)/(1+\alpha_0^2) \simeq 9$ GHz and the doubled frequency $2f_0 = 18$ GHz. As one can see from Fig. 1, the synchronization islands include field-only regime (h_s=0) and are "stacked" on top of each other along the h-axis. The number of the islands of synchronized motion is larger for the lower field frequencies, when magnetic moment can adjust to a different oscillation phase of the driving field. With the increase of f, the number of synchronization islands lowers but their area grow due to phase-locking synchronization phenomena that are